



HAL
open science

Primary break-up instabilities in a gas-liquid coaxial atomizer combined with electro-spray

R Osuna-Orozco, P D Huck, Nathanaël Machicoane, A. Aliseda

► **To cite this version:**

R Osuna-Orozco, P D Huck, Nathanaël Machicoane, A. Aliseda. Primary break-up instabilities in a gas-liquid coaxial atomizer combined with electro-spray. ICLASS 2018, 14th Triennial International Conference on Liquid Atomization and Spray Systems, Jul 2018, Chicago, United States. hal-02518493

HAL Id: hal-02518493

<https://hal.science/hal-02518493>

Submitted on 25 Mar 2020

HAL is a multi-disciplinary open access archive for the deposit and dissemination of scientific research documents, whether they are published or not. The documents may come from teaching and research institutions in France or abroad, or from public or private research centers.

L'archive ouverte pluridisciplinaire **HAL**, est destinée au dépôt et à la diffusion de documents scientifiques de niveau recherche, publiés ou non, émanant des établissements d'enseignement et de recherche français ou étrangers, des laboratoires publics ou privés.

Primary break-up instabilities in a gas-liquid coaxial atomizer combined with electro-spray

R. Osuna-Orozco*, P.D. Huck, N. Machicoane, A. Aliseda
Department of Mechanical Engineering, University of Washington, USA

Abstract

We present an experimental study that explores the combined physics of gas-assisted atomization and electro-sprays, based on a canonical coaxial gas-liquid atomizer. The laminar liquid stream is injected through a long straight metallic needle at the center of the turbulent gas jet. The needle is connected to a high-voltage source and the gas nozzle exit is grounded, creating a very strong electric field in which the dielectric liquid is charged up to approximately 0.1 – 1 Coulomb per kilogram. The gas momentum ratio varies from 0.9 to 80. The relative influence of the high-speed gas to the liquid electric charge on the primary instability and jet break-up is studied, using high speed visualizations in the near field, and in the mid field after break-up process has ended. The quantitative visualization captures the fast dynamics of the interface destabilization and clearly shows the changes in the liquid stream instabilities caused by the electric charge. These instabilities control the liquid droplet sizes and their spatio-temporal distribution in the spray. We apply an additional electric field along the spray development region, characterizing the ability of an external radial forcing to modify the structure of the spray in the mid field, by a study of the effect of control on the droplet number density, velocity and acceleration spatial distributions.

Introduction

Electrically charged sprays occur in many engineering applications, perhaps most notably in spray coating, mass spectrometry and fuel sprays for combustion. For many of these applications, liquid flows at low enough rates such that a Taylor cone can be formed and droplets are charged up to the Rayleigh limit [1]. However, there remain ample opportunities for the exploration of electro-hydrodynamics in sprays with higher flow rates where atomization is only partially driven by electrostatic repulsion [2] and where the charge is used in conjunction with an additional electric field downstream to tune the spray properties. The results presented here pertain to sprays formed using a canonical gas-liquid atomizer where atomization occurs due to a combination of electrostatic repulsion and high Reynolds number gas flow.

Experimental Methods

Experimental setup

A two-fluid coaxial atomizer has been designed to study atomization physics in a canonical setting. The design focuses on obtaining well-characterized and reproducible laminar liquid and turbulent gas streams. The liquid is introduced via a straight circular duct where a fully developed Poiseuille flow is the exit condition of the liquid into the atomization process. The gas is injected perpendicular to the axis of the gas nozzle through eight inlets (four on-axis inlets for the no-swirl gas feed, and four off-axis inlets for the swirl gas feed). It then develops along a nozzle whose inner (the outer wall of the liquid duct) and outer surfaces are shaped with cubic splines revolved around the axis of the injector (see [3] for more details on the design and the atomizer characterization). This canonical situation is also investigated using X-ray imaging and attenuation measurements [4, 5, 6] and computational simulations [7].

The momentum ratio $M = \rho_g U_g^2 / \rho_l U_l^2$ is based on the gas and liquid average velocity and density, $U_i = Q_i / A_i$ and ρ_i , where the subscripts g and l are used for gas and liquid respectively in the following, and A is the fluid area.

The needle is connected to a high-voltage source and the gas nozzle exit is grounded, creating a very strong electric field in which the dielectric liquid is charged up to approximately 0.1 – 1 C/kg (see figure 1). The gas momentum ratio varies from 0.9 to 80. An additional, approximately uniform (in the spray region), electric field can be applied using a parallel plate configuration (see [8]) to control the electrically charged spray.

High-speed shadowgraphy

This paper focuses on flow visualization that map the different modes of atomization accessible for study in this coaxial two-fluid atomizer with and without an applied voltage difference between the needle and nozzle tip.

*Corresponding author: roo3@uw.edu

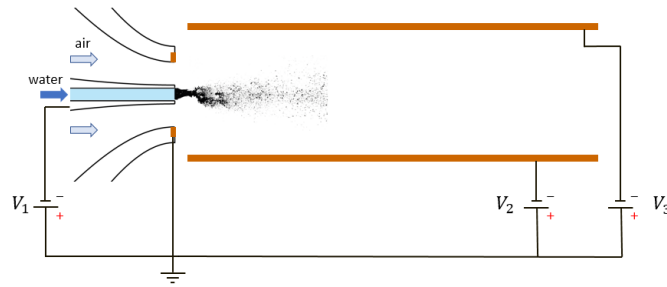


Figure 1. Schematics of the canonical coaxial two-fluid atomizer. The potential V_1 is set at -5 kV to charge the liquid, while the plate configuration can be $V_2 = V_3 = 0$ for outward electric forcing, $V_2 = V_3 = -5$ kV for an inward electric forcing and $V_2 = -5$ kV and $V_3 = 0$ for an upward electric forcing.

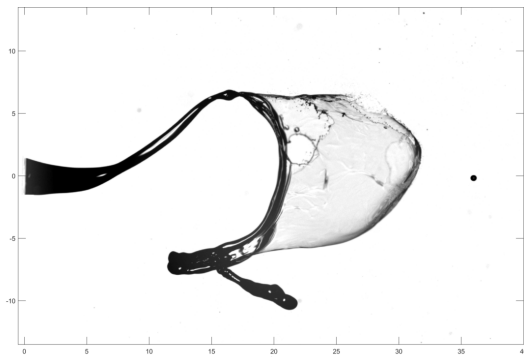


Figure 2. Shadowgraphy snapshot of flow at $Re_g = 10,627$ in the absence of applied voltage (scale is in mm).

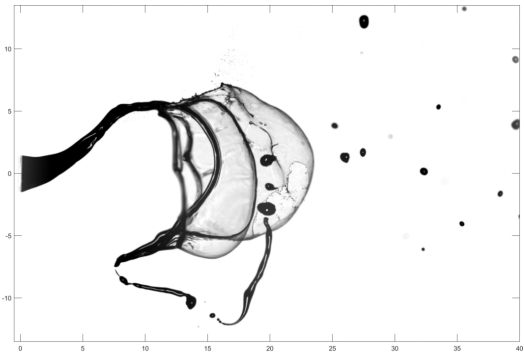


Figure 3. Shadowgraphy snapshot of flow at $Re_g = 10,627$ with 5 kV of applied voltage

Specifically, a range of gas Reynolds numbers from $10^4 - 2 \cdot 10^5$ has been explored, keeping the liquid Reynolds number constant at 1000 to maintain laminar conditions inside the liquid injection duct prior to the nozzle. This injection values result in gas-to-liquid momentum ratio ranging from $M = 0.9$ to 80. The Reynolds number is defined as $Re_i = 2Q_i / \sqrt{\pi A_i \nu_i}$, with Q and ν being the flow rate and the kinematic viscosity respectively.

Shadowgraphy high speed movies (912×912 pixels at 10,000 frames per second and 0.285 ns exposure time) allow for a quantitative mapping of the different instabilities and atomization modes [9]. At low gas Reynolds, $Re_g = 10^4$, and momentum ratio values, $M = 5$, a sinusoidal instability (referred to in the following as flapping) exposes the liquid jet to the high speed gas and results in multi-bag break up. At intermediate gas Reynolds numbers, the liquid jet accelerates, narrowing sharply within the potential cone of the gas, and suffers from a symmetric varicose instability that exposes the liquid to the high speed gas, with further instability, formation of ligaments and break up [10]. For the highest gas Reynolds numbers ($Re_g > 10^5$, $M > 70$), the liquid-gas interface is subject to the classical Kelvin-Helmholtz instability, the ligaments formed by this instability quickly accelerate and break into individual droplets due to the Rayleigh-Taylor instability of the liquid-gas interface[11].

Results and Discussion

We estimated the impact of the applied electric field on break-up instabilities using three metrics: flapping frequency, droplet size distribution and droplet area cover. Figures 2 and 3 show representative snapshots for the cases with and without an applied voltage. It is readily apparent that the presence of an electric field seems to increase the atomization efficiency with bag break-up occurring a shorter distance downstream (also occurring at a higher frequency as discussed below).

We characterize the primary break-up instability using power spectral densities of the light intensity of a radial profile spanning half of the jet at a position a few liquid diameters downstream from the nozzle. When one considers the sum of the light intensities along such a half-width of the spray, the flapping motions of the liquid core indeed induces drastic changes of this quantity over time, and its power spectral density (PSD) clearly shows peaks at the frequency of the liquid instability (figure 4). At low momentum ratios, the peak is well defined

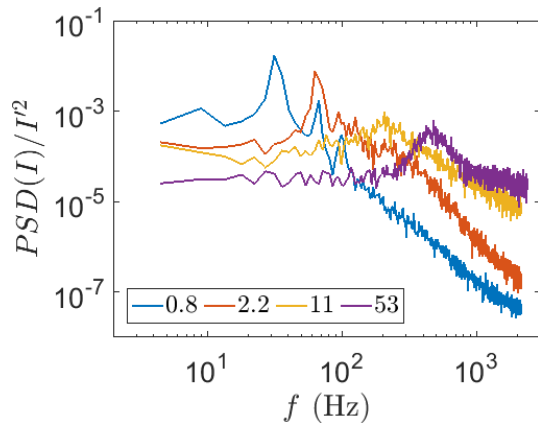


Figure 4. Power spectral density (PSD) of the pixel intensity summed along a cross-stream half-line for different values of the momentum ratio M , showing peaks at the flapping frequency.

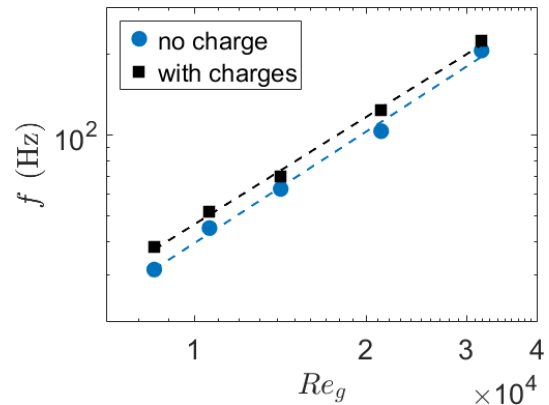


Figure 5. Flapping frequency, defined as the peak of the PSD from figure 4, as a function of the gas Reynolds number Re_g with (black) and without (blue) applied voltage.

and harmonics are present, while the peak moves to higher frequency values and broadens for higher M . Figure 5 shows the evolution of this flapping frequency with Re_g , which is well approximated by a power law with exponent 0.7. When a 5 kV potential difference is applied between the needle and the nozzle tip, the flapping frequency increases by a factor of about 1.2, while keeping a similar dependency on Re_g ; an observation that is consistent with increased atomization efficiency.

While shadowgraph high-speed movies are not suitable to measure the droplet size distribution after the secondary break-up occurs due to a lack of spatial resolution, it serves as a good estimate of the amount of fluid that is partially atomized after the primary break-up instability. Droplets are detected when they are in focus and above a certain threshold, and we considered an object to be a drop when its diameter is under the liquid diameter and when its shape meets certain sphericity criteria. Droplets size are measured on all 10,000 frames of a movie for each condition and the histogram obtained is normalized by the total number of frames where droplets are detected (figure 6). The droplet size distributions are approximated well by a decaying exponential function with rate of decay that increases as M increase. This enhanced decay is related to increased atomization of large drops into finer droplets. The droplet size distribution is modified slightly by the presence of an electric field, with the effect becoming less pronounced as the gas Reynolds number increases. In the presence of electric charge, shifts in the size distribution are consistent with a larger population of smaller diameter droplets.

Figure 7 shows the impact of a charged liquid stream on the amount of volume atomized within the field of view. For lower gas Reynolds numbers, the liquid atomized in the presence of electric charge covers an area of the image that is 4 times larger than the area covered by the atomized liquid when there is no electric charge. The differences between the two conditions decrease as the gas Reynolds number increases (to about 10% at the highest Re_g studied) and atomization is dominated by the momentum in the turbulent gas jet. Qualitatively, we observed that this increase in the break-up frequency and efficiency (smaller droplets formed at a faster rate), and which is detected in the quantitative analysis of the high speed images by the area covered by droplet, arises at least in part because ligaments break up more readily in the presence of electric charge.

Summary and Conclusions

We have demonstrated the impact of the applied electric field and liquid charging on break-up instabilities using three metrics: flapping frequency, droplet size distribution and droplet area cover. The presence of electric effects on the liquid phase consistently increased the frequency of the primary break-up instability of the jet for the range of gas Reynolds numbers explored. This observation was consistent with a measured increased in the volume of atomized liquid due to electrostatic effects. Furthermore, the presence of electric charge in the liquid resulted in a shift of the droplet size distribution, revealing an increase in the number of small diameter droplets in the spray.

The results presented here show that adding electric charge to the fluid in a gas atomizer can assist in the atomization especially at low gas Reynolds numbers. Addition of electric charge not only seems to improve atomization by increasing the fraction of the liquid that is atomized closer to the nozzle, and reducing the diameter

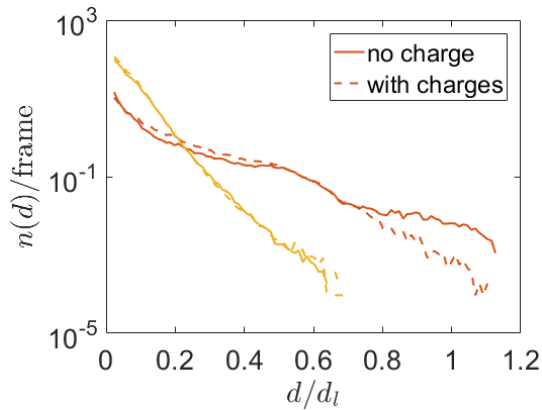


Figure 6. Histogram of the droplet size, normalized by the number of frames, in the shadowgraph movies, for $Re_g = 10, 600$ (red) and $Re_g = 10, 600$ (yellow) with and without an applied electric field.

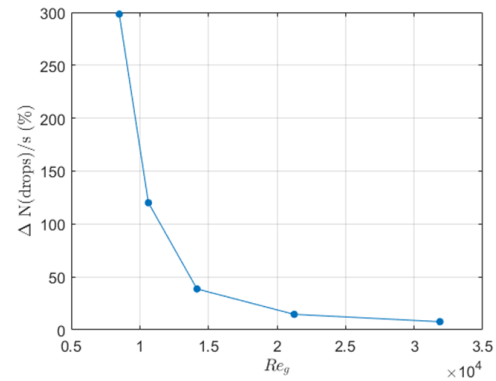


Figure 7. Percent difference in the area of the image covered by droplets for the cases with and without electric charge. The charged spray produces a larger volume of droplets (starting from the same volume of liquid), but the difference decreases at high Re_g .

of the resulting droplets, but also offers the opportunity to actuate on the spray dispersion using external electric fields. This characteristics of the gas-liquid coaxial atomizer combined with electro-spray make it an appealing actuation strategy to add to the toolbox available for feedback control of conventional two-fluid atomizers.

Acknowledgements

This work was sponsored by the Office of Naval Research (ONR) as part of the Multidisciplinary University Research Initiatives (MURI) Program, under grant number N00014-16-1-2617. The views and conclusions contained herein are those of the authors only and should not be interpreted as representing those of ONR, the U.S. Navy or the U.S. Government.

References

- [1] Ganan-Calvo, A. *Scientific Reports* 6, Scientific reports., Vol.6. (2016).
- [2] Li, G., Luo, X., Si, T., Xu, R. X., Li, Guangbin, Luo, Xisheng, Si, Ting, Xu, Ronald X. *Physics of Fluids* 26(5), 054101 (2014).
- [3] Huck P., Machicoane N., Osuna R., Aliseda A., *14th Triennial International Conference on Liquid Atomization and Spray Systems*, Chicago, Illinois, July 22-26, 2018.
- [4] Bothell, J. K., Li, D., Morgan, T. B., Heindel, T. J., Aliseda, A., Machicoane, N., Kastengren, A., *14th Triennial International Conference on Liquid Atomization and Spray Systems*, Chicago, Illinois, July 22-26, 2018.
- [5] Li, D., Bothell, J. K., Morgan, T. B., Heindel, T. J., Aliseda, A., Machicoane, N., Kastengren, A., *14th Triennial International Conference on Liquid Atomization and Spray Systems*, Chicago, Illinois, July 22-26, 2018.
- [6] Morgan, T. B., Bothell, J. K., Li, D., Heindel, T. J., Aliseda, A., Machicoane, N., Kastengren, A., *14th Triennial International Conference on Liquid Atomization and Spray Systems*, Chicago, Illinois, July 22-26, 2018.
- [7] Vu, L. X., Chiodi, R., Desjardins, O. *14th Triennial International Conference on Liquid Atomization and Spray Systems*, Chicago, Illinois, July 22-26, 2018.
- [8] Machicoane N., Osuna R., Aliseda A., *14th Triennial International Conference on Liquid Atomization and Spray Systems*, Chicago, Illinois, July 22-26, 2018.
- [9] Marmottant, P., Villermaux E., *Journal of Fluid Mechanics* 498:73-111 (2004).
- [10] Lasheras, J. C., Hopfinger, E. J., *Annual Revue of Fluid MEchanics*, 32:275-308 (2000)
- [11] Aliseda, A., Hopfinger, E. J., Lasheras, J. C., Kremer, D. M., Berchielli, A., Connolly, E. K., *International Journal of Multiphase Flow* 34(2):161-175 (2008).